

NUMERICAL MODELING OF SEDIMENT TRANSPORT IN HARBORS AND STUDY OF PLANFORM EFFECTS ON SEDIMENTATION

M.Mojabi^(a), K.Hejazi^(b), M.Mohammadi Aragh^(c)

^(a)M.Sc. Student, K.N.Toosi University of Technology, Tehran, Iran

^(b)Faculty Member, K.N.Toosi University of Technology, Tehran, Iran

^(c)Senior Engineer, Integrated Hydro-Environment Research Group, K.N.Toosi University of Technology, Tehran, Iran

^(a)Moien.Mojabi@gmail.com, ^(b)Hejazik@kntu.ac.ir, ^(c)MohammadiM@ihr.ir

ABSTRACT

Sedimentation is a common problem in many harbors, which requires frequent dredging and involves considerable maintenance costs. Consequently harbor planform, which influences flow pattern, plays a crucial role in sedimentation in harbors. In this study a 2DH finite volume numerical model including sediment transport module has been developed and utilized to investigate the effects of harbor planform on sedimentation in harbors.

Keywords: Sediment transport, Harbor Planform, 2DH, sedimentation

1. INTRODUCTION

Sedimentation reduces the required navigation depth in harbors and disturbs vessels passage. In order to provide safe passage for vessels, maintenance dredging which is the most expensive item in running costs of harbors is necessary. The amount of maintenance dredging depends on the sedimentation rate in harbor basin and therefore, minimizing the depth reduction in harbors is one of the most important criteria in harbor design.

Generally, sediments transported to harbors by currents and waves are deposited in parts of the harbor where currents and waves are not strong enough to keep sediments in motion, which results in the sediment deposition and reduction of water depth.

2. HYDRODYNAMIC AND SEDIMENT TRANSPORT MODEL

A two dimensional depth-averaged numerical model including hydrodynamic and sediment transport module has been developed herein.

Hydrodynamic module predicts horizontal depth-averaged velocities and water surface elevation, solving shallow water equations. Finite volume technique has been utilized for discretization of the equations. In order to solve the resulting system of equations, the Alternating Direction Implicit (ADI) method has been employed.

Sediment transport module predicts suspended sediment concentration and bed level changes by solving well known depth-averaged advection-diffusion

and sediment mass balance equations respectively. In order to estimate sediment erosion and deposition rate, Krone (1962) and Partheniades (1965) formulas are used respectively.

Hydrodynamic and sediment transport modules are coupled under the basic assumption that during hydrodynamic computations the bed elevation remains constant and similarly, hydrodynamic conditions do not change during bed level calculations. Moreover, it is assumed that suspended sediment load has no effect on hydrodynamic conditions in corresponding time step.

2.1. Hydrodynamic Module

Shallow water set of equations including effects of turbulence and bottom stress are represented as follows (Liggett 1994):

$$\frac{\partial h}{\partial t} + \frac{\partial(uh)}{\partial x} + \frac{\partial(vh)}{\partial y} = 0 \quad (1)$$

$$\begin{aligned} \frac{\partial(uh)}{\partial t} + \frac{\partial(uuh)}{\partial x} + \frac{\partial(vuh)}{\partial y} = & -gh \frac{\partial(h+z_b)}{\partial x} \\ & + \frac{1}{\rho} \frac{\partial(hT_{xx})}{\partial x} + \frac{1}{\rho} \frac{\partial(hT_{xy})}{\partial y} - \frac{\tau_{bx}}{\rho} \end{aligned} \quad (2)$$

$$\begin{aligned} \frac{\partial(vh)}{\partial t} + \frac{\partial(uvh)}{\partial x} + \frac{\partial(vvh)}{\partial y} = & -gh \frac{\partial(h+z_b)}{\partial y} \\ & + \frac{1}{\rho} \frac{\partial(hT_{yx})}{\partial x} + \frac{1}{\rho} \frac{\partial(hT_{yy})}{\partial y} - \frac{\tau_{by}}{\rho} \end{aligned} \quad (3)$$

where u and v are depth-averaged horizontal velocities in x and y direction respectively, h is water depth, and z_b is bed elevation, T_{xx} , T_{xy} , T_{yx} , T_{yy} are depth-averaged turbulent stresses, τ_{bx} , τ_{by} are bed shear stresses in x and y direction respectively, ρ is water density and g is the gravity acceleration.

Bed shear stresses are determined using simple quadratic friction law as represented by Eq (4). Here C is chezy coefficient.

$$\begin{bmatrix} \tau_{bx} \\ \tau_{by} \end{bmatrix} = \rho \frac{g}{C^2} \sqrt{u^2 + v^2} \begin{bmatrix} u \\ v \end{bmatrix} \quad (4)$$

Turbulent shear stresses are calculated using simple Boussinesq assumption, (Rodi, 1993):

$$\begin{aligned} T_{xx} &= 2\rho v_t \left(\frac{\partial u}{\partial x} \right), & T_{yy} &= 2\rho v_t \left(\frac{\partial v}{\partial y} \right) \\ T_{xy} &= T_{yx} = \rho v_t \left(\frac{\partial u}{\partial y} + \frac{\partial v}{\partial x} \right) \end{aligned} \quad (5)$$

Where v_t is turbulent eddy viscosity and may be calculated using depth-averaged parabolic model, (Rodi, 1993) as represented by Eq (6). Here α is an empirical coefficient. In present study α is set to 0.2.

$$v_t = \alpha u_* h \quad u_* = c_f \sqrt{u^2 + v^2} \quad c_f = \frac{\sqrt{g}}{C} \quad (6)$$

2.2. Suspended Sediment Transport Module

In the case of fine sediment transport, bed load is a negligible part of total load transport and in the present study is not taken into account.

Sediment transport module calculates the suspended sediment concentration solving depth-averaged advection-diffusion equation, (Zhou and Lin ,1998):

$$\begin{aligned} \frac{\partial(ch)}{\partial t} + \frac{\partial(uch)}{\partial x} + \frac{\partial(vch)}{\partial y} &= \frac{\partial}{\partial x} \left(\varepsilon_x h \frac{\partial(c)}{\partial x} \right) \\ &+ \frac{\partial}{\partial y} \left(\varepsilon_y h \frac{\partial(c)}{\partial y} \right) + E_b - D_b \end{aligned} \quad (7)$$

Where c is the depth-averaged concentration, ε_x , ε_y are sediment diffusion coefficients in x and y direction respectively, E_b is sediment erosion rate, and D_b is sediment deposition rate. Sediment erosion and deposition rates are estimated using Krone (1962) and Partheniades (1965) formulas as represented by Eq (8) and Eq (9) respectively.

$$D = \begin{cases} w_s c \left(1 - \frac{\tau_b}{\tau_{cd}}\right) & \text{for } \tau_b < \tau_{cd} \\ 0 & \text{for } \tau_b > \tau_{cd} \end{cases} \quad (8)$$

$$E = \begin{cases} M \left(\frac{\tau_b}{\tau_{ce}} - 1 \right) & \text{for } \tau_b > \tau_{ce} \\ 0 & \text{for } \tau_b < \tau_{ce} \end{cases} \quad (9)$$

Where τ_b is bed shear stress, τ_{cd} critical stress for deposition, τ_{ce} critical stress for erosion, w_s settling velocity, and M erosion constant.

Krone (1962), proposed following formula for cohesive sediment settling velocity

$$w_s = 0.001C^{4/3} \quad (10)$$

where C is suspended sediment concentration (gr / lit)

Bed level changes are calculated using sediment mass balance equation (Eq.11):

$$(1-n) \frac{\partial z}{\partial t} = -(E_b - D_b) \quad (11)$$

where n is bed materials porosity.

2.3. Discretization of Equations

The governing equations are discretized using finite volume method on a rectangular uniform grid with staggered variable arrangements.

Equations (1, 2, 3 and 7) are integrated over control volume shown in Fig (1). Convective terms are discretized using third order TVD, SDPUS-C1 scheme (Lima et al., 2010). Using first order backward scheme for time derivative terms and second order central difference scheme for diffusive terms, discretized equations may be written in the form of Eq (12). Resulting system of equations is solved using ADI technique.

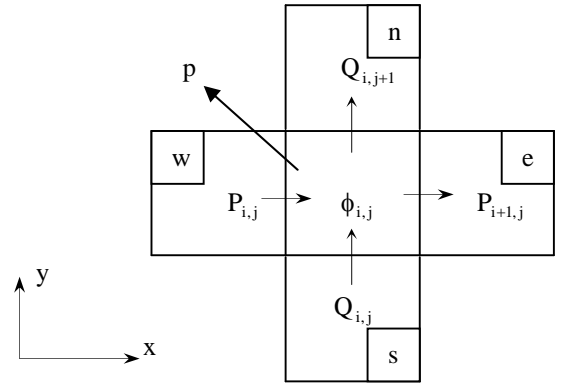


Figure (1) Two dimensional cartesian grid where ϕ stands for h, c and z . n, e, w, s are indexes for neighboring cells. p is an index for central cell.

$$\begin{aligned} A_p H_{i,j}^{n+1} + A_e P_{i+1,j}^{n+1} + A_w P_{i,j}^{n+1} + A_n Q_{i,j+1}^{n+1} + A_s Q_{i,j}^{n+1} &= 0 \\ B_e P_{i+1,j}^{n+1} + B_e H_{i+1,j}^{n+1} + B_p H_{i,j}^{n+1} &= R_p^n \\ C_n Q_{i,j+1}^{n+1} + C_n H_{i,j+1}^{n+1} + C_p H_{i,j}^{n+1} &= R_Q^n \\ F_p C_{i,j}^{n+1} + F_e C_{i+1,j}^{n+1} + F_w C_{i-1,j}^{n+1} + F_n C_{i,j+1}^{n+1} + F_s C_{i,j-1}^{n+1} &= R_C^n \end{aligned} \quad (12)$$

where $P = uh$, $Q = vh$.

3. MODEL VALIDATION

3.1. Hydrodynamic Module

In this paper experimental data of stationary free surface flow in a square cavity (Langendoen, 1992) are used for model verification. The flow into the square harbor is driven by a constant discharge of $u_h = 0.042 \text{ m}^2 / \text{s}$ per width in the main channel. Initial water depth was set to 0.11 m. In the physical model, channel length was 18m, but in numerical simulations the length of channel is reduced to 5m (Hakimzadeh 2004) in the favor of saving computational time. The computational domain configuration is represented in Fig (1). Numerical predictions and experimental results compared in Fig (2) show a good agreement. Another test simulates, a subcritical flow over a bump (Goutal and Maurel, 1997). In this simulation discharge per width and initial water elevation in the channel are $4.42 \text{ m}^2 / \text{s}$ and 2 m respectively. Numerical prediction and analytical solution obtained from Bernoulli's theorem show good agreement as shown in Fig (3).

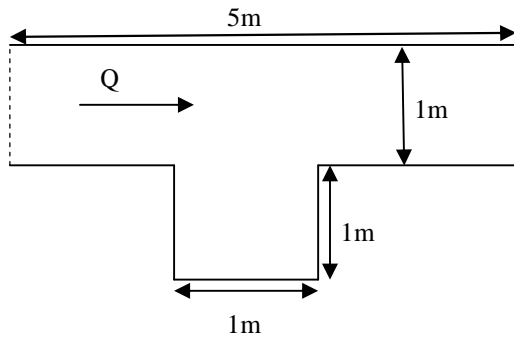


Figure (1) Numerical model configuration

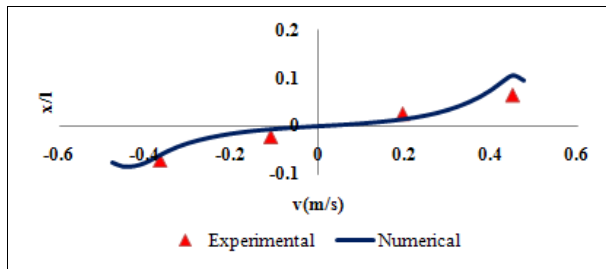


Figure (2a) Comparison of velocity of flow across x axis

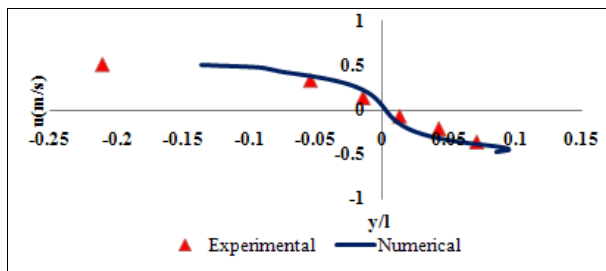


Figure (2b) Comparison of velocity of flow across y axis

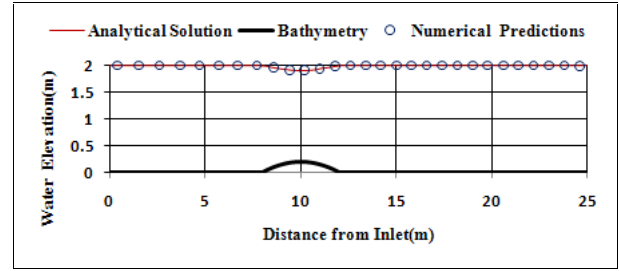


Figure (3) Water elevation (subcritical flow over a bump)

3.2. Sediment Transport Module

To evaluate sediment transport module combined advection-diffusion Transport and sediment mass conservation are examined. Results demonstrate model capabilities in solving advection-diffusion equations and maintaining sediment mass conservation accurately.

3.2.1. Combined Advection-Diffusion Test

Wexler (1992), proposed analytical solution, to the advection-diffusion equation including source-sink terms (Eq.12). Boundary and initial conditions are presented by Eq (13). Velocity profile and diffusion coefficients are assumed to be constant over computational domain. Equation (14) reads the analytical solution.

$$\frac{\partial(ch)}{\partial t} + \frac{\partial(uch)}{\partial x} + \frac{\partial(vch)}{\partial y} = \frac{\partial}{\partial x} \left(\epsilon_x h \frac{\partial(c)}{\partial x} \right) + \frac{\partial}{\partial y} \left(\epsilon_y h \frac{\partial(c)}{\partial y} \right) - \lambda c \quad (12)$$

$$\begin{aligned} c &= c_0 \quad \text{for } x=0 \quad \text{and } y_1 < y < y_2 \\ c &= 0 \quad \text{for } x=0 \quad \text{and } y_1 > y \quad \text{or } y > y_2 \\ \frac{\partial c}{\partial x} &= 0 \quad \text{for } x=L, \quad \frac{\partial c}{\partial y} = 0 \quad \text{for } y=0 \\ \frac{\partial c}{\partial y} &= 0 \quad \text{for } y=W \\ c &= 0 \quad \text{for } 0 < x < L, \quad \text{and } 0 < y < W \\ P_n &= \frac{y_1 - y_2}{W} \quad \text{for } n=0 \\ P_n &= \frac{\sin(\eta y_1) - \sin(\eta y_2)}{n\pi} \quad \text{for } n \neq 0 \end{aligned} \quad (13)$$

where L = length of domain and W = width of domain Results for unit depth, $u = 1 \text{ ft/day}$, $v = 0 \text{ ft/day}$, $k_x = 200 \text{ ft/day}^2$, $k_y = 60 \text{ ft/day}^2$, $\lambda = 0.001$ are shown in Fig(4), that confirm the accuracy of advection -diffusion simulation. In the figure, red lines represent analytical solution and contours show numerical prediction.

$$c(x, y, t) = c_0 \sum_0^{\infty} L_n P_n \cos(\eta y) \times \left\{ \exp\left(\frac{x(U-\beta)}{2k_x}\right) \operatorname{erfc}\left(\frac{x-\beta t}{2\sqrt{k_x t}}\right) + \exp\left(\frac{x(U+\beta)}{2k_x}\right) \operatorname{erfc}\left(\frac{x+\beta t}{2\sqrt{k_x t}}\right) \right\} \quad (14)$$

$$\beta = \sqrt{U^2 + 4k_x(\eta^2 k_y + \lambda)}$$

$$\eta = \frac{n\pi}{W}, \quad n = 0, 1, 2, \dots$$

$$L_n = 0.5 \quad \text{for } n = 0, \quad L_n = 1 \quad \text{for } n > 0$$

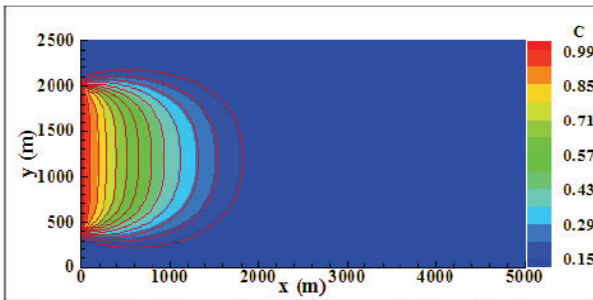


Figure (4) A Comparison of numerical prediction and analytical solution to the advection-diffusion equation.

3.2.2. Sediment Mass Conservation Test

To evaluate model capabilities in simulating sediment transport, a numerical simulation of sediment transport on a rectangular domain with a simple sloped bottom has been carried out as reported by Pandoe et al. (2004) and demonstrated in Figure (5a) and (5b). Except for critical shear stresses for erosion and deposition, other parameters are same as those used by Pandoe et al. (2004). The flow boundary condition with the discharge of $uh = 2.50 \text{ m}^2/\text{s}$ per width is imposed on the left hand boundary and the water elevation is kept constant ($\eta = 0$) on the right hand side. Other two boundaries are land boundaries. The computational domain is 12 km long and 4 km wide. After 24 hours the simulation is stopped. To maintain sediment mass conservation, of net erosion (erosion + deposition) should equal to the sum of suspended sediment volume in water column and sediment volume that leaves the channel from open right boundary. Fig (6a) and (6b) show suspended sediment concentration in water column and bed erosion/deposition along the centerline of the channel. Results presented in Table (1) shows an error of only 2% for sediment mass conservation simulation. The source of error is the accumulative numerical errors that come from discretization and the solution of hydrodynamic and sediment transport equations.

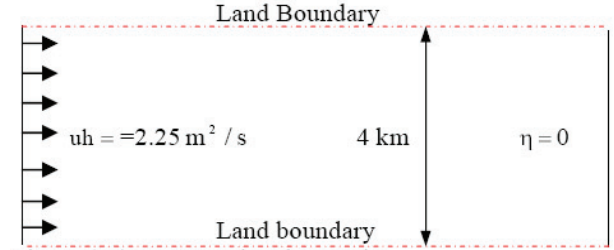


Figure (5a) Computational Domain

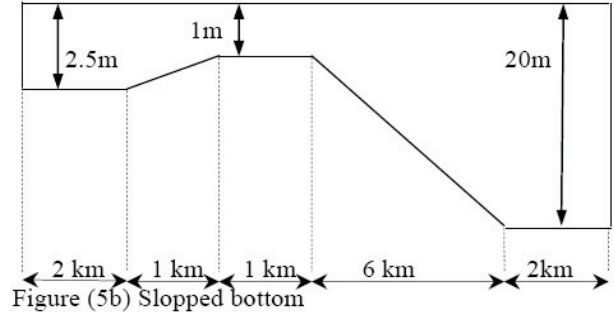


Figure (5b) Sloped bottom

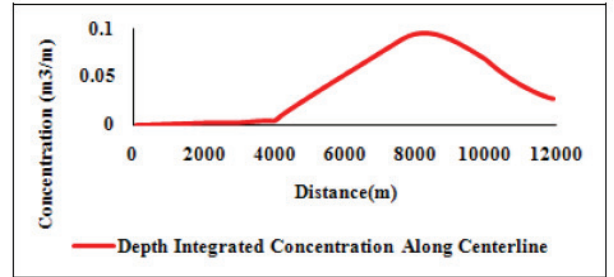


Fig (6a) Suspended Sediment Concentration Per Unit Width along Channel

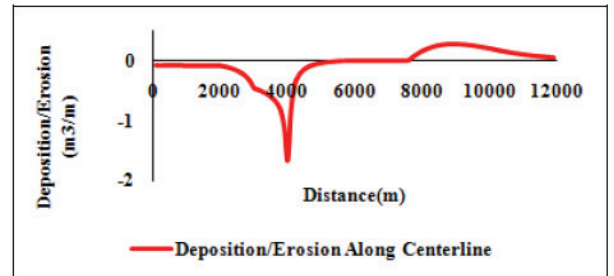


Fig (6b) Erosion/Deposition Per Unit Width along Channel

Table (1) Sediment mass conservation results

Net Erosion	Suspended sediment	Sediment inflow	Sediment outflow	Error
2450 m ³	1820 m ³	0 m ³	639.95 m ³	%2.0

4. PLANFORM INVESTIGATION

Sediments are transported into the harbor basin and deposited when the flow is no longer capable of keeping sediments in suspension. Therefore the flow characteristics play an important role in suspended sediment transport and deposition pattern in harbor basin.

Flow in the harbor basin is driven by flow in main channel and one or more eddies depending on harbor geometry form in the harbor (Kuijper et al., 2005). Flow separation occurs at upstream corner of the basin and a turbulent mixing layer forms between harbor basin and main channel flow (Winterwerp, 2005), as shown in Fig (7).

Amount of sediment exchange that occurs between harbor basin and main channel depends on strength of turbulent mixing layer between harbor and main channel which is also influenced by harbor geometry (Winterwerp, 2005 and Kuijper et al., 2005). Therefore, in addition to flow characteristics, harbor planform affects sediment exchange between harbor and main channel to a high extent.

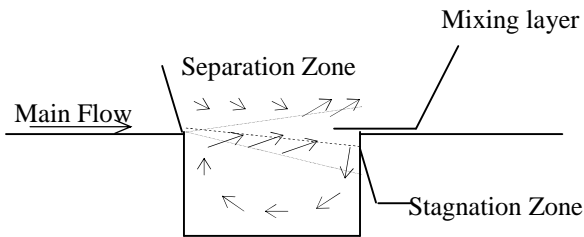


Figure (7): Schematic form of mixing zone (Kuijpe et al., 2005)

In this study, to investigate the planform effects on sedimentation in harbors a wide range of aspect ratios for rectangular harbors with constant area of 2.25 m^2 have been examined in the numerical model. In all simulations, flow discharge and the still water depth are set to $0.042 \text{ m}^2/\text{s}$ per width and 0.11 m respectively, as has been demonstrated in Langendoen (1992). Zero water elevation imposed at the right open boundary and the suspended sediment concentration at the left boundary is set to $10 \text{ kg}/\text{m}^3$. Initial suspended sediment concentration is $0.6 \text{ kg}/\text{m}^3$.

Critical shear stress for deposition is reported between 0.05 and $0.1 \text{ N}/\text{m}^2$ (Self et al., 1986). Parchure and Mehta (1985) reported values for τ_{ce} between 0.04 and $0.62 \text{ N}/\text{m}^2$. Reported values for M coefficient lies between 0.00001 and $0.0005 \text{ kg}\cdot\text{m}^{-2}\cdot\text{s}^{-1}$ (Van Rijn, 1993).

After 30 minutes simulation is stopped and net deposition in the harbor basin is the measure for which, comparison has been considered. Other simulation parameters and geometry of numerical model are presented in Table (2) and Fig (8) respectively.

Table 2 Numerical simulation parameters

Inflow m^2/s	τ_{ce} N/m^2	τ_{cd} N/m^2	C $\text{m}^{0.5}/\text{s}$	M $\text{kg}\cdot\text{m}^{-2}\cdot\text{s}^{-1}$
0.042	0.2	0.05	90	0.00001

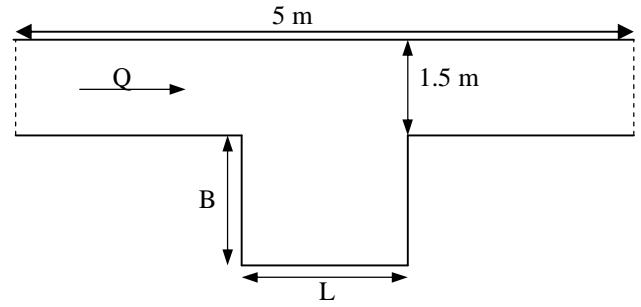


Figure (8) Numerical simulation geometry

5. RESULTS AND DISCUSSION

Simply, it may seem that reducing harbor mouth necessarily leads to sedimentation reduction in the harbor, but it is not exactly the case. Although, the wider harbor mouth may possibly lead to more suspended sediment exchange between harbor and main channel, but on the other hand, it results in stronger flow in the harbor basin, so, the hydrodynamic characteristics in the harbor have to be taken into account. Sedimentation volume against aspect ratio is plotted as seen in Fig (9).

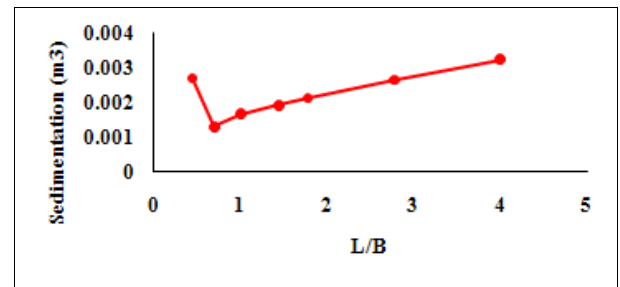


Fig (9): Aspect ratio effect on sedimentation volume

As indicated by results, for $L/B < 0.7$, although increasing harbor mouth leads to increase in suspended sediment exchange between harbor and channel, but stronger flow reduce deposition in the harbor. So as long as $L/B < 0.7$, the flow is dominant factor in sedimentation in harbor. Similarly for $L/B > 0.7$, it can be observed that sediment exchange across the harbor is more important. In addition, it can be observed that for square harbors ($L/B=1$), the sedimentation volume per unit area is decreased with increasing harbor length, Fig (10)

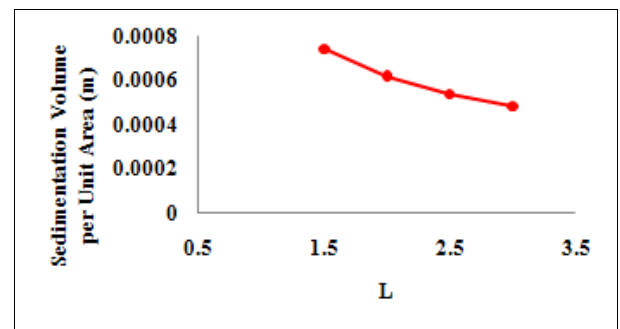


Fig (10): Dimension effect on sedimentation volume per unit area in Square harbors

6. CONCLUSION

A numerical hydrodynamic and sediment transport model has been developed herein. The model has been validated against both experimental and numerical results which confirm the accuracy of predictions.

In this study planform effects on sedimentation in the harbor basin is investigated by examination of a range of aspect ratios varying from 0.44 to 4.0. For $L/B < 0.7$ flow characteristics play a more important role in sedimentation whereas, for $L/B > 0.7$, sediment exchange between harbor and channel is a more dominant factor. Moreover, in order to minimize sedimentation in the square harbor, the aspect ratio should be kept as close to 0.7 as possible.

REFERENCES

- Goutal, N., and Maurel, F. 1997. Simulation, Direction des études et recherches. *Proceeding of, 2nd Workshop on Dam-BreakWave*, Electricité de France, Rep. HE43/97/016/B.
- Lima, G.A.B., Corrêa, L., Candezano, M.A.C., Sartori, P. and Ferreira, V.G., 2010. A Simple NVD/TVD-Based Upwinding Scheme for Convection Term Discretization. *Proceeding V European Conference on Computational Fluid Dynamics*, ECCOMAS CFD, June 14-17 (Lisbon, Portugal)
- Hakimzadeh, H., 2004. Second-Order Closure Study of River-Harbour Flow. *Iranian Journal of Science & Technology*, Transaction B, 28 (B5)
- Krone, R.B., 1962. Flume experiments of transport of sediments in estuarial processes. Final Report, H.E.L.S.E.R.L., Univ. of California, Berkeley, California DA-04-203, CIVENG-59-2
- Kuijper, C., Christiansen, A.J., Cornelisse, J.M., Winterwerp, C., 2005. Reducing harbor siltation. II: Case study of Parkhafen in Hamburg. *Journal of Waterway, Port, Coastal, and Ocean Engineering-ASCE*, 131 (6), 267– 276
- Langendoen, E., 1992. *Flow patterns and transport of dissolved matter in tidal harbours*, Thesis (PhD). Delft University of Technology, Delft, The Netherlands
- Liggett, J.A., 1994. *Fluid Mechanics*, McGraw-Hill, Inc.
- Parchure, T.M. and Mehta, A.J., 1985. Erosion of soft cohesive sediment deposits. *Journal of Hydraulic Engineering-ASCE*, 111 (10), 1308– 1326
- Partheniades, E., 1965. Erosion and deposition of cohesive soils. *Journal of hydraulic engineering*, ASCE, 9 (HY1)
- Rodi, W., 1993. *Turbulence models and their application in hydraulics*. 3rd Ed., IAHR Monograph, Balkema, Rotterdam, The Netherlands.
- Self, R.F.L., Nowell, A.R.M. and Jumars, P.A. 1986. Factors controlling critical shear for deposition and erosion of individual grains. *Marine Geology*, 86, 181-199
- Van Rijn, L.C., 1993. *Principles of sediment transport in rivers, estuaries and coastal seas*. Amsterdam, The Netherlands, Aqua Publications
- Pandoe, W.W. and Edge, B.L., 2004. Cohesive sediment transport in the 3D hydrodynamic baroclinic circulation model. *Ocean Engineering* 31, 2227–2252
- Wexler, E.J., 1992. Analytical solutions for one-, two- and three dimensional solute transport in ground-water system with uniform flow, USGS report, Techniques of water-resources investigations of the United States geological Survey, Chapter B.7, United States government printing office.
- Winterwerp, C., 2005. Reducing harbor siltation. I: Methodology. *Journal of Waterway, Port, Coastal, and Ocean Engineering-ASCE*, 131 (6), 258– 266
- Zhou, J. and Lin, B. 1995. 2D Mathematical Model for Suspended Sediment, Part 1: Model Theory and Validations. *Journal of Basic Science and Engineering*, 3, (1),